Colloids and Surfaces B: Biointerfaces 172 (2018) 423–429

Contents lists available at ScienceDirect

Colloids and Surfaces B: Biointerfaces

journal homepage: www.elsevier.com/locate/colsurfb

Phase-segregated membrane model assessed by a combined SPR-AFM approach

M. Antonieta Daza Millone[a,*], Romina F. Vázquez[b], Sabina M. Maté[b], María E. Vela[a]

[a] Instituto Nacional de Investigaciones Fisicoquímicas Teóricas y Aplicadas (INIFTA), CCT- La Plata, CONICET, Universidad Nacional de La Plata, Sucursal 4 Casilla de Correo 16, La Plata, 1900, Argentina

[b] Instituto de Investigaciones Bioquímicas de La Plata (INIBIOLP), CCT- La Plata, CONICET, Facultad de Ciencias Médicas, Universidad Nacional de La Plata, 60 y 120, La Plata, 1900, Argentina

ARTICLE INFO

Keywords:
Supported lipid bilayer
Surface plasmon resonance
Force spectroscopy
Biomimetic systems
Cyclodextrin
Raft-like domains

ABSTRACT

Model biomembranes can provide valuable insights into the properties of complex biological membranes. Among several techniques, Surface Plasmon Resonance (SPR) provides a label-free analysis of the interactions of bioactive molecules with biomembranes with an experimental setup that allows mimicking biological environments. Nevertheless, protocols that enable the preparation of stable supported membrane systems with reproducible structural and functional properties on the biosensor chip are still needed. In this work, we present a simple protocol to modify SPR substrates that allows the formation of a phase-segregated supported lipid bilayer (SLB). SLBs are formed by fusion of lipid vesicles of pure phospholipids (DMPC, DPPC and DOPC) and of a ternary mixture (DOPC/16:0 SM/Cho in 2:1:1 molar ratio) on a SPR gold sensor chip covered with a dithiothreitol monolayer. The formation of a SLB on the SPR sensing surface in a reproducible way was assessed by the combined use of the SPR technique with AFM. The interaction of a cholesterol-extracting drug with SLBs was studied as a model of membrane-lipophilic biomolecule interaction. The proposed strategy allowed us to obtain a membrane model where phase coexistence is present and where Cho depletion from ternary mixtures was comparable to the extraction results reported for human erythrocytes.

1. Introduction

Cell membranes are the single barrier separating the intracellular environment from the extracellular space, in which several kinds of biological functions take place, namely, mechanical, electrical, signaling and transport functions. It is nowadays recognized that the investigation of the nanoscopic organization of membranes that controls their mechanical properties is meaningful not only to clarify most biological events but also to utilize them in advanced applications [1–3], such as drug screening [4,5], biosensors [6] and biomimetic separation [7]. However, biological cell membranes are very complex systems, and consequently the investigation of their structure and functions is not straightforward. Therefore, model biomembranes can provide valuable insights into the properties of complex biological membranes [8]. The lipid bilayer composition of these artificial membranes can be easily controlled by the preparation conditions. Several techniques were developed for analyzing membrane model systems at both the microscopic and the molecular levels. Among them, Surface Plasmon Resonance (SPR) has evolved into an exciting technique in the label-free analysis of biomolecular interactions, allowing high-throughput screening of the structural and compositional factors that mediate the binding of bioactive molecules to the membrane [9]. The SPR experimental setup allows mimicking the biological environment where the interaction process under study takes place. Nevertheless, protocols that enable the preparation of stable supported membrane systems with reproducible structural and physicochemical properties on the biosensor chip are still needed.

The self-assembly of supported lipid bilayers (SLBs) from vesicles in solution is the most versatile, simple and reproducible method to prepare continuous and almost defect-free fluid bilayers [10,11]. Several factors influence the results such as the surface properties, the lipid composition, size and solution composition of the vesicles, the osmotic pressure and the temperature [12]. However, liposomes interact weakly and do not rupture on unmodified gold surfaces, except for the case of Au (111) substrates [13,14]. Indeed, the mechanism of vesicle spreading on Au (111) was described in depth by Pawlowski et al. [15] On the contrary, SPR substrates are polycrystalline and require surface modification to enable vesicle adsorption and eventual fusion [3,11].

* Corresponding author.
E-mail address: dazamillone@inifta.unlp.edu.ar (M.A. Daza Millone).

https://doi.org/10.1016/j.colsurfb.2018.08.066
Received 19 June 2018; Received in revised form 9 August 2018; Accepted 29 August 2018
Available online 31 August 2018

Highly hydrophilic films or adlayers, such as SiO_2 [11,16], self-assembled monolayers [3,17] and polymer cushions [11,16,18], are frequently employed to modify gold substrates to achieve free standing bilayers. If this direct strategy fails, due to the inherent system properties, lipophilic anchors [19,20] can be added to enhance the adhesion or derivatized molecules such as thiophospholipids [18,21,22] or specific thiolated linkers (avidin/biotin, [23,24] His-Tag, and nucleotides [25]) can be employed. Another resource consists of employing detergents [26], PEG solution [23] or fusion peptides [10,27], adding washing steps to avoid remains of these agents. It is evident that increasing the chip complexity not only demands more preparation time and the use of expensive reagents but drifts the model further away from the native membrane limiting its versatility. Among the questions that could arise are whether the SPR substrate allows vesicle fusion or only their adsorption, or a mixture of both [16]; if there is a good coverage or if the compound under study is interacting with the surface [28] and whether there is a way to control and characterize the mechanical properties of the bilayer. Regarding this last point, it is noteworthy that the composition and the lateral organization, i.e. the presence of segregated domains or "lipid raft-like domains", in the lipid bilayer interface play a critical role in studies of ligand-receptor interactions on membranes. The effective exposure of ligand moieties [29], the secondary structure of peptides [30], the interaction with nanoparticles [31] and the triggering of cell responses [32], among others, have been reported to be influenced by phase-segregation studies with SLBs.

In this work, we present a simple protocol to modify SPR gold substrates that allows the formation of SLBs of a ternary lipid mixture (DOPC/SM 16:0/Cho) that exhibits phase coexistence, i.e. a liquid-ordered (L_o) phase enriched in sphingomyelin (SM) and cholesterol (Cho) which is segregated from the liquid-disordered (L_d) phase composed mainly of DOPC [33,34]. SLBs were formed by vesicle fusion on dithiothreitol (DTT) self-assembled monolayers (SAMs) on Au following previous procedures [35,36]. The presence of different lipid phases was characterized by means of atomic force microscopy (AFM), a powerful technique that enables imaging in a liquid environment [37]. Furthermore, force spectroscopy (FS) gives information about the nanomechanical properties and distribution of lipid phases in SLBs [38–40]. This technique is of particular importance since the evidence of the lipid bilayer formation cannot be directly demonstrated in a polycrystalline substrate [21].

Here, we present the first use of a combined SPR-AFM approach to prepare and characterize membrane-mimetic surfaces with lipid raft-like domains, and we demonstrate the ability of AFM to determine the topological and nanomechanical properties of the membrane on a SPR sensor chip. These lipid phases formed on the polycrystalline gold were comparable to the ones obtained on a flat mica substrate. The combination of these techniques allowed us to corroborate the adequate formation of a SLB as a model of membrane-lipophilic biomolecule interactions for SPR studies. The PC/SM/Cho lipid mixture, that mimics the outer leaflet of human erythrocytes, was exposed to methyl-β-cyclodextrin (MβCD), a Cho-extracting drug. Cho depletion from ternary mixtures was comparable to the extraction results reported for human red blood cells.

2. Material and methods

2.1. Reagents and materials

1,2-Dimyristoyl-sn-glycero-3-phosphocholine (DMPC), 1,2-dipalmitoyl-sn-glycero-3-phosphocholine (DPPC), 1,2-Dioleoyl-sn-glycero-3-phosphocholine (DOPC), N-palmitoyl-D-erythro-sphingosylphosphorylcholine (16:0 SM) and cholesterol (Cho) were purchased from Avanti Polar Lipids (Birmingham, AL, USA). DL-Dithiothreitol (DTT), methyl-β-cyclodextrin (MβCD), N-(2-Hydroxyethyl)piperazine-N′-(2-ethanesulfonic acid) (HEPES) and other reagents, all analytical-grade, were purchased from Sigma Aldrich (St. Louis, MO, USA) and Tris base from J. T. Baker (Center Valley, PA, USA). Chloroform and methanol, HPLC-grade, were purchased from Merck (Darmstadt, Germany). The ultrapure MilliQ water (MerckMillipore, Burlington, WI, USA) used for all the solutions and experiments had a resistivity of 18.2 MΩ cm at 23 °C.

Gold evaporated (~50 nm) on glass substrates (SPR102-AU) were obtained from Bionavis (Tampere, Finland). Muscovite mica grade V-1 was purchased from SPI Supplies (West Chester, PA, USA).

2.2. Vesicle preparation

Multilamellar vesicles (MLVs) were prepared from synthetic pure lipids (DMPC, DPPC and DOPC) dissolved in chloroform. The ternary mixture (TM) was prepared by mixing appropriate amounts of DOPC, 16:0 SM and Cho (2:1:1 molar ratio, respectively) and then dissolved in chloroform/methanol (2:1, v/v). Each sample was dried by evaporating the solvent under a stream of N_2 and placed at high vacuum for 2 h in a glass chamber connected to a vacuum pump. The samples were hydrated in PBS (10 mM Na_2HPO_4, 1.8 mM KH_2PO_4, 137 mM NaCl, 2.7 mM KCl pH 7.0), Tris (20 mM Tris base, 150 mM NaCl pH 7.4) or HEPES (25 mM HEPES, 150 mM NaCl pH 7.4) buffers and stirred to facilitate dispersion. After completing lipid detachment from the bottom of the test tube, MLVs were introduced in a bath sonicator (TB04TA, Testlab, Argentina) and kept at 65 °C (for DPPC and TM) for 1 h. In this way, small unilamellar vesicles (SUVs) were generated.

2.3. DTT-gold substrate preparation

SPR gold substrates were washed with hot (~70 °C) ammonia-peroxide solution (30% NH_3: 100 vol H_2O_2:H_2O 1:1:2) for a couple of minutes, rinsed with ultrapure water and absolute ethanol and dried with N_2. Immediately, the substrates were immersed in ethanolic 50 μM DTT solution for 30 min in the absence of light (covered with aluminum foil). As previously reported [35], this procedure was optimized to achieve a fully covered gold surface with only one monolayer of DTT. After thoroughly rinsing with absolute ethanol, substrates were dried with a stream of N_2.

2.4. SPR measurements

SPR measurements were performed in Kretschmann configuration using a BioNavis Navi™ 200 (MP-SPR) device (Tampere, Finland) equipped with two independent lasers (670 and 785 nm) in a dual-channel system. Measurements were made in angular-scan mode (40–78 degrees), recording SPR curves every 3.5 s at a constant temperature of 23 °C.

Ex- situ prepared DTT-gold substrates were placed in the flow chamber and washed with high buffer flux (500 μL/min) and 1% Triton X-100 aqueous solution (1 min at 50 μL/min). Vesicle suspensions (0.1–1 mg/mL) were injected at 10 μL/min with times ranging from 15 to 40 min. Unbound vesicles were washed with high buffer flux and 1-min injection of 100 mM NaOH solution at 50 μL/min. The amount of immobilized lipid was recorded after 10 min of signal stabilization, the angular shifts reported are the mean value of at least 5 independent experiments. DTT-gold surfaces were regenerated with two consecutive 1-min injections of 1% Triton X-100 aqueous solution at 50 μL/min before a fresh vesicle suspension was injected.

MβCD binding measurements were performed using 30-min injection of MβCD solution (0.25, 0.5, 1 and 3 mM) in Tris buffer for the ternary mixtures. For each MβCD solution assessed, a fresh lipid sample was prepared and the amount of lipid immobilized was normalized to 1.0, in order to compare the amount of extracted cholesterol. Control experiments with DMPC were performed and as already reported [41] no material was extracted (see *Supporting information* Fig S1).

2.5. AFM measurements

Ex-situ lipid samples were prepared in mica and DTT-gold substrates. Before vesicle contact, a 5 µL drop of $CaCl_2$ 1 mM was added to freshly cleaved mica. After 15 min of interaction time, the surface was carefully washed with MilliQ water. Then, 100 µL of vesicle suspensions were dropped on mica and allowed to interact for 1 h at 23 °C for DMPC and 60 °C for the ternary mixture. The same procedure was employed for DTT-gold samples but the temperature was kept at 23 °C for both samples. Excess of lipid vesicles was washed with buffer solution and the samples were placed in the AFM fluid chamber without drying.

AFM measurements were performed on a multimode atomic-force microscope controlled by a Nanoscope-V unit (Veeco Instruments Inc., USA). V-shaped Si_3N_4 probes (Veeco Instruments Inc., USA) with spring constants of 0.06-0.18 N/m were used in contact and tapping mode. Individual spring constants were calibrated using the equipartition theorem (thermal tune) [42] and the piezo sensitivity (V/nm) was measured. All the experiments were carried out at a temperature of 23 °C in a fluid cell. Resolution images of 512 × 512 pixels were collected at a scanning rate between 0.5 and 1 Hz. The height and error-signal (vertical deflection) images were taken simultaneously. Images were analyzed with Gwyddion software [43].

Force-volume (FV) maps were acquired from 3 µm x 3 µm images with arrays of 16 × 16 force curves at scan rates of 1 Hz and tip velocity of 400–600 nm/s. The rupture forces were extracted from the FV maps with an own routine developed in MatLab software with a NanoScope utility. The routine script is available in SI.

3. Results and discussion

3.1. Interaction of lipid vesicles with DTT monolayers on SPR gold sensor

Lipid vesicles of pure phospholipids (DMPC, DPPC, DOPC) and a ternary mixture (DOPC/16:0 SM/Cho in 2:1:1 molar ratio) were allowed to interact with a SPR gold sensor chip covered with a dithiothreitol (DTT) monolayer (Fig. 1).

DTT-Au surfaces have proven to be adequate to obtain substrates fully covered with DMPC bilayers by vesicle fusion in HEPES pH 7.4 buffer at 37 °C [35,36]. However, SPR equipments are not often prepared to make *in situ* experiments with temperature gradients [44], since laser alignment and calibration are affected. Vesicle adsorption, rupture, fusion and the phase state of SLBs are also strongly influenced by temperature [12].

In the present work, different conditions were assayed in order to achieve a surface fully covered with a lipid bilayer at a constant temperature of 23 °C. For this purpose, single lipids that present different phase state at 23 °C DMPC (T_m = 24 °C), DPPC (T_m = 41 °C) and DOPC (T_m = −17 °C) were used together with a ternary lipid mixture (hereafter referred as TM) in which lipid phase coexistence is observed with liquid ordered domains (L_o) enriched in SM and Cho immersed in a liquid disordered (L_d) phase. This TM was the main purpose of our study as it is widely used as a mammalian membrane model system [33,45]. Another point to highlight is that we aimed to a system that was easy to regenerate for successive experiments and the possibility of reusing the same chip. After each assay the lipids were completely removed with 1 min injection of Triton X-100 1% and DTT monolayers can be removed with NH_3 35%:H_2O_2 100 vol:H_2O (1:1:2) immersion at ~ 90 °C to achieve a clean gold surface without changes in surface grain morphology nor plasmon absorption.

Measurements made with PBS pH 7.0 running buffer (Fig. 1a) show large shifts in the minimum angle of the SPR curve (Θ_{min}) for the TM while DMPC, DPPC and DOPC vesicles produce smaller shifts for the same time of interaction (20 min) and vesicle concentration (0.2 mg/mL). Longer interaction times (up to 40 min), higher concentrations (up to 1 mg/mL) and/or multiple vesicle solution injections increase the final change in Θ_{min} achieving values of $\Delta\Theta_{min}$ ~ 0.4. Divalent cations, i.e. Ca^{2+}, are frequently employed to enhance vesicle fusion because of their ability to produce conformational changes in the headgroups and order the acyl chains [46]. Since Ca^{2+} and phosphate ions generate insoluble salts, PBS was switched to Tris (Fig. 1b) and HEPES running buffers with 3 mM Ca^{2+} addition. With similar results, both Tris-Ca^{2+} and HEPES-Ca^{2+} (from hereafter we will present results in Tris-Ca^{2+} buffer) allowed us to yield higher $\Delta\Theta_{min}$ values for DMPC and DPPC but only a slight increase for DOPC. On the contrary, the TM shows a decrease in $\Delta\Theta_{min}$ compared to values obtained in PBS, reaching a mean value of 0.65 ± 0.05, even with longer interaction times (up to 40 min). For the pure phospholipids, multiple injections yield higher values of $\Delta\Theta_{min}$ (~ 0.5), with injection times up to 1 h.

At this point, the question that arises is whether a high $\Delta\Theta_{min}$ in SPR measurements represents a better coverage or not, i.e. if after the vesicle fusion, homogenous bilayers or patchy lipid multilayers are formed. Surface coverage can be estimated through the de Feijter equation [47], which relates the surface density (Γ_p) of the layer to the refractive indexes (RI) of a layer (n_p) and the medium (n_m), the refractive index increment (dn/dc) and the layer thickness (d_p):

$$\Gamma_p = \frac{(n_p - n_m)d_p}{dn/dc} \quad (1)$$

The shifts in $\Delta\Theta$ are proportional to the changes in RI [48] :

$$n_p - n_m = \Delta n = \Delta\Theta * k \quad (2)$$

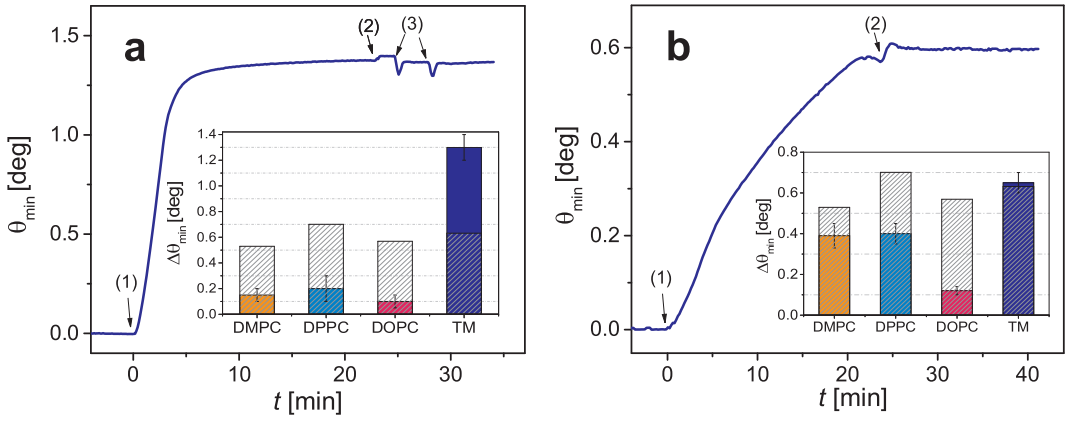

Fig. 1. Interaction of lipid vesicles with DTT-Au surfaces. Lipid vesicle suspensions (0.2 mg/mL) were injected at 10 µL/min into: a) PBS pH 7.0 and b) Tris-Ca^{2+} (3 mM) pH 7.4 running buffers. The injection start (1) and end (2) as well as the washing procedure with 500 µL/min flux (3), are marked with arrows. Sensorgrams show the shift in minimum angle of SPR curve (Θ_{min}) for ternary mixtures (TM: DOPC/16:0 SM/Cho 2:1:1). The insets summarize the net changes $\Delta\Theta_{min}$ and their corresponding theoretical values for bilayer coverage (colored and dashed filled bars, respectively) for DMPC, DPPC, DOPC and TM.

Table 1
Angular shifts ($\Delta\Theta$) calculated from mean molecular area (mma) and RI increment (dn/dc) reported values.

Lipid	mma [Å^2]	Γ_p [ng/cm^2]	dn/dc	$\Delta\Theta$ [deg]
DMPC	59.5 [50]	378.4	0.1398 [51]	0.5294
DPPC	48 [50]	507.9	0.138 [52]	0.7009
DOPC	67 [33]	389.7	0.146 [52]	0.5689
TM	56 [45]	394.7	0.16 [53]	0.6315

where the constant k is the sensitivity coefficient for the instrument. Taking into account Eqs. (1) and (2), $\Delta\Theta$ can be expressed as:

$$\Delta\Theta = \frac{\Gamma_p\,(dn/dc)}{k * d_p} \tag{3}$$

For thin films (< 100 nm), $k{*}d_p$ is approximately constant [49], and for aqueous buffers in contact with Au sensors at 670 nm of laser wavelength in SPR Navi200 this value is 1.0×10^{-7} nm/degree. Taking into account the mean molecular area (*mma*) of each lipid and the reported values of *dn/dc*, the theoretical angular shifts were calculated for a full bilayer coverage (Table 1).

Marked differences between the theoretical and the experimental values can be seen in the insets of Fig. 1. In PBS buffer, the pure lipids, i.e., DMPC, DPPC and DOPC, do not reach the calculated values for full coverage while for the TM the experimental value exceeds it. This $\Delta\Theta_{min}$ excess persists after washing procedures with high flux buffer (500 µL/min) or with NaOH 0.1 M solution and could be assigned to unfused adsorbed vesicles. For the same injection time and lipid concentration, Tris-Ca^{2+} running buffer seems to improve the coverage and shows a better match with the calculated value for TM. Nevertheless, it is necessary to further inquire whether the data correspond to a complete lipid bilayer or to adsorbed vesicles. We will discuss this issue in the next section.

3.2. Force spectroscopy of DMPC and ternary mixture surfaces

In order to assess the nature of the lipid coverage we employed AFM as a complementary technique to the SPR measurements. Cross-sectional AFM data are able to confirm the typical thickness of lipid bilayers formed in plane substrates, *e.g.,* mica [37] or Au (111) [54], by vesicle fusion. On the contrary, when the lipid bilayer conformally covers a nanostructured rough surface as the DTT-Au sensor, the cross section analysis is difficult or impossible to perform [21]. However, force spectroscopy is a powerful tool that provides information on the nanomechanical properties of supported lipid bilayers [39,40] and can be used to elucidate if the lipids adsorb as entire vesicles, bilayers or a mixture of them [55]. In this technique, a topographic characterization of the surface by AFM imaging is followed by a Force-Volume (FV) mapping of the same area (see Fig. S2 in SI). FV maps consist in force-distance curves taken in a grid of a selected zone. Bilayer covered areas exhibit ruptures at characteristic breakthrough force values (F_B).

First, we analyzed a simple membrane model consisting of pure DMPC, which has been widely characterized [35,36,56] and will be useful to compare results between mica and SPR substrates before assessing the TM model. The DMPC samples obtained by vesicle fusion on mica and DTT-gold substrates were prepared *ex- situ* in Tris-Ca^{2+} buffer. AFM images and the statistical distribution of F_B are shown in Fig. 2a and b.

The cross sections of DMPC bilayers in mica substrate (Fig. 2a) were used to obtain their mean thickness which is in good agreement with reported values of free standing DMPC bilayers [35,40]. The topography of the DMPC covered DTT-Au surface (Fig. 2c) is not very different from that of the bare DTT-Au, both with typical values of root mean square roughness (rms) of 1.4–2.0 nm. FV maps (Fig. 2b and d) were obtained from multiple scans of the same zone in 3 µm x 3 µm areas and yield F_B mean values of 6.4 ± 0.1 nN and 5.6 ± 0.1 nN for DMPC on mica and DTT-Au substrates respectively. These results are in agreement with reported values for DMPC bilayers on mica at the same ionic strength [38], and they are an average of different zones of the same sample and were corroborated in at least 5 different samples. The difference in the mean values between them can be related to variations in different samples and AFM probes, which can be up to 15–20 % [38]. In both cases, only 65–70 % of all the analyzed curves had rupture events while the other curves resembled the ones obtained for the bare substrate. In addition, force-distance curves can be transformed into force-separation curves to determine the bilayer thickness (see Fig. S2d in SI) [57]. The estimated thickness of DMPC bilayers on mica and DTT-Au gold substrates were 4.8 ± 0.3 nm and 4.7 ± 0.4 nm, respectively. These values are consistent with cross section measurements on mica substrates (Fig. 2a) and provide additional evidence of the bilayer formation.

In contrast to DMPC, TM bilayers show phase domain segregation with ~ 0.5 nm height differences between the liquid disordered (L_d) and liquid ordered (L_o) domains (Fig. 3a). Correspondingly, the F_B histograms (Fig. 3b) exhibit two distributions with maximums at 4.79 ± 0.01 nN and 12.32 ± 0.03 nN, consistent with previous reports [33]. The topographic images of DTT-Au substrates covered with the TM do not show any feature that can be related to phase coexistence (Fig. 3c). Nevertheless, the F_B histograms (Fig. 3d) also have two components with mean values of 5.14 ± 0.07 nN and 12.4 ± 0.1 nN which confirm that TM characteristics on the DTT-Au surface and on the mica surface are similar regarding the phase segregation. For both cases, the rupture events were found in 89–94 % of the curves analyzed. These values arose from different zones of the same sample and were corroborated in at least 5 different samples.

Despite the difference in the full width at half maximum (FWHM) of the F_B distributions on mica and DTT-Au substrates, their mean values are very similar for both DMPC and TM, revealing the same nanomechanical properties in both substrates. Thus, one can infer that the bilayers are formed on DTT-Au and are compositionally and structurally similar to those formed on mica.

Ex-situ AFM experiments made in PBS in the absence of Ca^{2+} at 23 °C for the TM, showed adsorbed vesicles on mica substrates (see Fig. S3 in SI). FV maps were taken in this condition and, in this case, the force-distance curves show very scarce rupture events (< 1.5–2%) at F_B > 1 nN with the same setup conditions as the previous experiments. Events at lower values (< 1 nN) were similar to those reported for adsorbed vesicles [55], and were not further analyzed. These results reinforced the idea that the larger $\Delta\Theta_{min}$ obtained for these mixtures compared to the corresponding theoretical $\Delta\Theta_{min}$ calculated for a full surface coverage (Fig. 1 and Table 1) could arise from the adsorption of the lipid vesicles in absence of vesicle fusion when no Ca^{2+} is present.

3.3. Interaction of a cholesterol-extracting drug with ternary mixture bilayers

Through AFM experiments we were able to confirm the presence of a TM bilayer with the expected structural characteristics (L_o/L_d phases) formed on the SPR sensor chip and with nanomechanical properties that match those obtained for the supported TM bilayer in mica. In order to test whether SPR measurements with the TM supported on the DTT-Au chip were suitable to study biomolecular interactions with mammalian membranes, Cho-extraction assays, a frequently applied method to reduce the amount of Cho in cellular membranes, were performed. The removal of Cho from the lipid bilayer induces alterations in membrane biophysical properties, leading to significant membrane reorganization and, consequently, disruption of several cell functions and signaling [58]. The use of cyclodextrins and their derivatives is the mostly chosen method to lower the Cho levels of cellular membranes and lipid model systems [28,59]. Taking into account that Cho removal from erythrocytes by methyl-β-cyclodextrin (MβCD) is

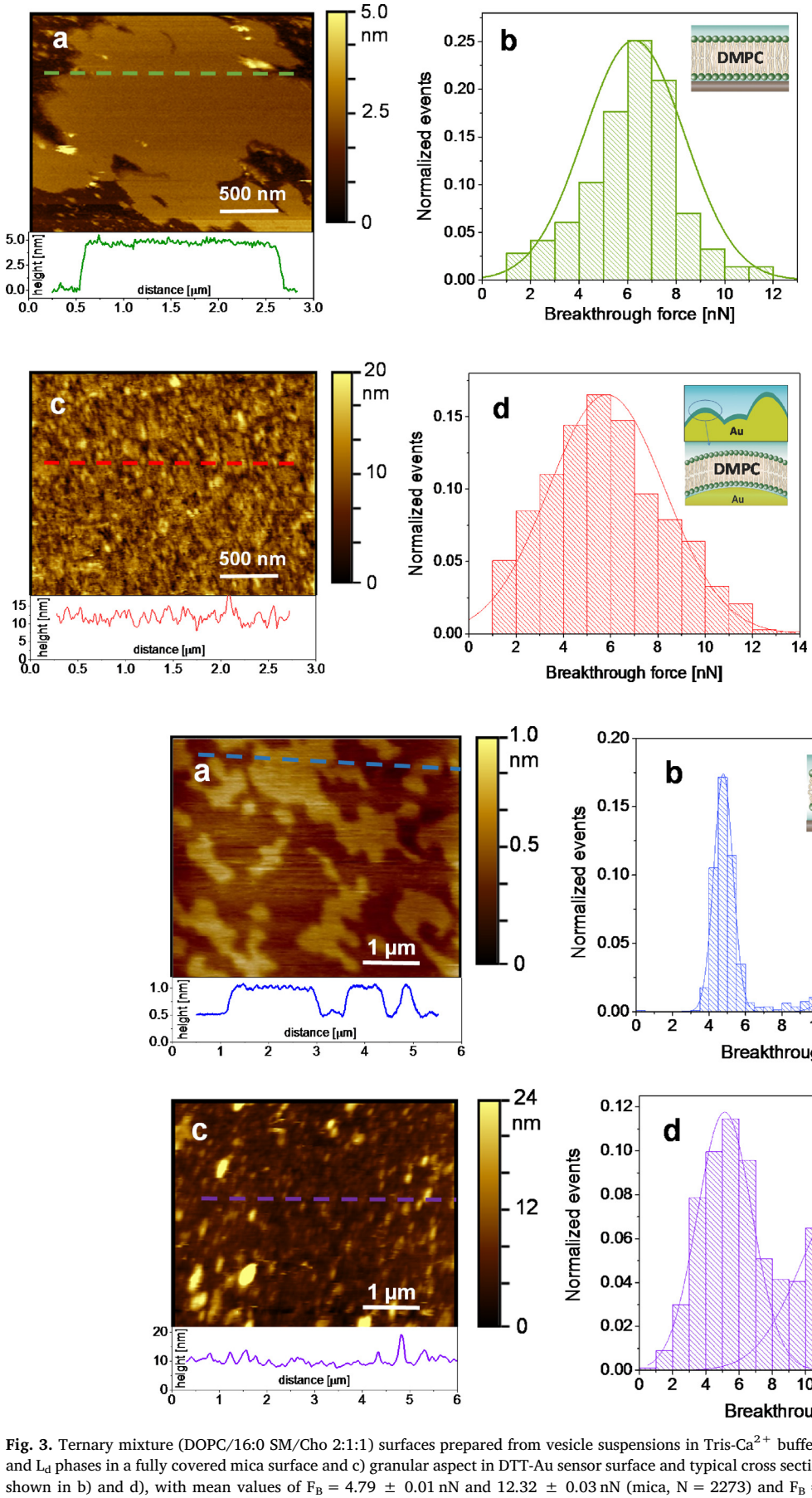

Fig. 2. DMPC surfaces prepared from vesicle solution in Tris-Ca^{2+} buffer pH 7.4. AFM images show: a) flat extended covered regions of DMPC bilayers on mica and c) grained aspect of DTT-Au surface after DMPC vesicle fusion. Below, typical cross sections taken at the slashed lines. b) and d) breakthrough force (F_B) distributions taken at different regions of the surface in 3 µm x 3 µm, with mean values of F_B = 6.4 ± 0.1 nN (mica, N = 1055) and F_B = 5.6 ± 0.1 nN (DTT-Au, N = 1344). Gaussian distribution curves for F_B data are shown as solid lines.

Fig. 3. Ternary mixture (DOPC/16:0 SM/Cho 2:1:1) surfaces prepared from vesicle suspensions in Tris-Ca^{2+} buffer pH 7.4. AFM images show: a) coexistence of L_o and L_d phases in a fully covered mica surface and c) granular aspect in DTT-Au sensor surface and typical cross sections taken at the slashed lines. F_B distributions are shown in b) and d), with mean values of F_B = 4.79 ± 0.01 nN and 12.32 ± 0.03 nN (mica, N = 2273) and F_B = 5.14 ± 0.07 nN and 12.4 ± 0.1 nN (DTT-Au, N = 1807). Solid lines are Gaussian distribution fits for the F_B data.

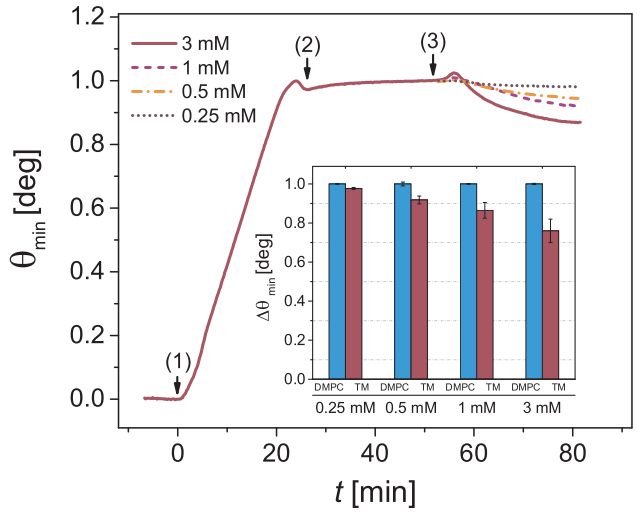

Fig. 4. Interaction of methyl-β-cyclodextrin (MβCD) with ternary mixtures (DOPC/16:0 SM/Cho 2:1:1). The sensorgram shows the start (1) and end (2) of injection of the vesicle suspension. Plateau values were normalized to 1. The injection of MβCD started at (3) and continued for 30 min. Final values for each concentration of MβCD assayed (0.25, 0.5, 1 and 3 mM) are depicted in the inset and compared with DMPC as control surface.

well described in the literature [60], we prepared TM bilayers with the previously optimized conditions described in the first section and after a stabilization period of 20 min we injected MβCD (Fig. 4). For each MβCD concentration assayed, a fresh bilayer was prepared and in order to normalize the results, every plateau was brought to 1. MβCD was allowed to interact for 30 min and the final Θ_{min} values reached are shown in the *inset* of Fig. 4 where they are compared to data obtained for control experiments with DMPC.

According to previous reports [41], MβCD does not interact with pure DMPC in the concentration range tested (0.25-3 mM MβCD). The signal increase during the association step but the baseline is fully recovered at the end of the injection time (see Fig. S1 in SI). Even for the highest concentration, there was no extraction of material from the surface nor adsorption of MβCD (neither onto DMPC SLBs nor in patches or discontinuities of that layer). These results suggest that there are no matrix effects in the DTT-Au system, unlike those reported for commercial chips [28], where lipophilic anchors can interact with MβCD.

In the case of TM, a slight increase in the signal is observed at the beginning of the association step, due to MβCD injection, and then a decrease, proportional to the concentration of MβCD assayed and reflecting the Cho depletion from the TM. The decrease is significant for MβCD concentrations above 0.25 mM and for the highest concentration tested (3 mM MβCD), the amount of removed material reached 24%, which is consistent with reported values for human erythrocytes in isotonic solution [60]. Furthermore, the Cho extraction profiles followed a biexponential decay model (see Fig. S4 in SI), that has been widely described in presence of raft-like domains, i.e. Cho is depleted from two different phases (L_d and L_o) [28,59,61,62].

These results showed that the protocol we performed allowed us to prepare a model membrane with phase segregation on a SPR sensor chip suitable for the study of molecular interactions. In particular, kinetic analysis of Cho extraction is of outmost importance in physiological or pharmacological studies where the mechanisms involved are closely related to the activity (escape tendency) of Cho, for instance, the mechanism of action of the anesthetics and the function of neuronal receptors, channels and transporters [62].

4. Conclusions

SPR gold substrates can be easily modified with a DTT monolayer that enables vesicle fusion of pure (DMPC) and ternary lipid mixtures (DOPC/SM 16:0/Cho 2:1:1) in Tris-Ca^{2+} buffer. This approach does not require washing steps and the substrates did not show unspecific binding issues. AFM imaging of these SPR samples along with force spectroscopy (FS) revealed that the ternary mixture exhibits phase segregation with breakthrough force (F_B) values comparable with the same SLB on mica. In order to verify whether this membrane model was suitable for studies in human red blood cells, a Cho-extracting drug was employed. The results show that the percentage of Cho release bears close resemblance to the one reported for erythrocytes.

This approach to form and characterize an SLB on SPR substrates may be useful for immobilizing a broad number of amphiphiles and for advanced applications of SLBs. Not only the composition is certain but also the organization and nanomechanical properties can be evaluated, such as the presence of lipid rafts or their continuity, *e.g.*, success of the vesicle fusion process in producing a continuous supported bilayer on the DTT-Au sensor chip surface for biomolecule-membrane studies.

Acknowledgements

We thank Mario Raúl Ramos for the graphic designs. This work was supported by the Agencia Nacional de Promoción Científica y Tecnológica [PICT 2016-0679], CONICET PIP 2015-2017 No 112, 201501, 0671 CO, the Universidad Nacional de La Plata [M11/191] and [11/X760]. M.A.D.M. and S.M are members of the Carrera del Investigador of CONICET. R.V. is a researcher of the Universidad Nacional de La Plata (UNLP), Argentina. M.E.V, is a member of the Carrera del Investigador CICBA, Argentina.

Appendix A. Supplementary data

Supplementary material related to this article can be found, in the online version, at doi:https://doi.org/10.1016/j.colsurfb.2018.08.066.

References

[1] Y.-R. Kim, S. Jung, H. Ryu, Y.-E. Yoo, S.M. Kim, T.-J. Jeon, Synthetic biomimetic membranes and their sensor applications, Sensors (2012) 12.
[2] C.H. Nielsen, Biomimetic membranes for sensor and separation applications, Anal. Bioanal. Chem. 395 (2009) 697–718.
[3] E.T. Castellana, P.S. Cremer, Solid supported lipid bilayers: from biophysical studies to sensor design, Surf. Sci. Rep. 61 (2006) 429–444.
[4] P.B. Bennett, H.R.E. Guthrie, Trends in ion channel drug discovery: advances in screening technologies, Trends Biotechnol. 21 (2003) 563–569.
[5] A. Smith, Screening for drug discovery: the leading question, Nature 418 (2002) 453.
[6] B.A. Cornell, V.L.B. Braach-Maksvytis, L.G. King, P.D.J. Osman, B. Raguse, L. Wieczorek, R.J. Pace, A biosensor that uses ion-channel switches, Nature 387 (1997) 580.
[7] A. van Oudenaarden, S.G. Boxer, Brownian ratchets: molecular separations in lipid bilayers supported on patterned arrays, Science 285 (1999) 1046.
[8] R. Glazier, K. Salaita, Supported lipid bilayer platforms to probe cell mechanobiology, Biochim. Biophys. Acta 1859 (2017) 1465–1482.
[9] M.A. Cooper, Advances in membrane receptor screening and analysis, J. Mol. Recognit. 17 (2004) 286–315.
[10] G.J. Hardy, R. Nayak, S. Zauscher, Model cell membranes: techniques to form complex biomimetic supported lipid bilayers via vesicle fusion, Curr. Opin. Colloid Interface Sci. 18 (2013) 448–458.
[11] R.P. Richter, R. Bérat, A.R. Brisson, Formation of solid-supported lipid bilayers: an integrated view, Langmuir 22 (2006) 3497–3505.
[12] E. Reimhult, F. Höök, B. Kasemo, Intact vesicle adsorption and supported biomembrane formation from vesicles in solution: influence of surface chemistry, vesicle size, temperature, and osmotic pressure, Langmuir 19 (2003) 1681–1691.
[13] J.T. Marques, R.F.M. de Almeida, A.S. Viana, Biomimetic membrane rafts stably supported on unmodified gold, Soft Matter 8 (2012) 2007–2016.
[14] M. Li, M. Chen, E. Sheepwash, C.L. Brosseau, H. Li, B. Pettinger, H. Gruler, J. Lipkowski, AFM studies of solid-supported lipid bilayers formed at a au(111) electrode surface using vesicle fusion and a combination of langmuir – blodgett and langmuir – schaefer techniques, Langmuir 24 (2008) 10313–10323.
[15] J. Pawłowski, J. Juhaniewicz, A. Güzeloğlu, S. Sęk, Mechanism of lipid vesicles spreading and bilayer formation on a Au(111) surface, Langmuir 31 (2015)

11012–11019.
[16] N. Granqvist, M. Yliperttula, S. Välimäki, P. Pulkkinen, H. Tenhu, T. Viitala, Control of the morphology of lipid layers by substrate surface chemistry, Langmuir 30 (2014) 2799–2809.
[17] C. Sandoval-Altamirano, S.A. Sanchez, N.F. Ferreyra, G. Gunther, Understanding the interaction of concanavalin a with mannosyl glycoliposomes: a surface plasmon resonance and fluorescence study, Colloids Surf. B Biointerfaces 158 (2017) 539–546.
[18] C. Rossi, J. Chopineau, Biomimetic tethered lipid membranes designed for membrane-protein interaction studies, Eur. Biophys. J. 36 (2007) 955–965.
[19] C.L. Baird, E.S. Courtenay, D.G. Myszka, Surface plasmon resonance characterization of drug/liposome interactions, Anal. Biochem. 310 (2002) 93–99.
[20] M.A. Cooper, A.C. Try, J. Carroll, D.J. Ellar, D.H. Williams, Surface plasmon resonance analysis at a supported lipid monolayer, Biochim. Biophys. Acta 1373 (1998) 101–111.
[21] A. Kılıç, M. Fazeli Jadidi, H.Ö. Özer, F.N. Kök, The effect of thiolated phospholipids on formation of supported lipid bilayers on gold substrates investigated by surface-sensitive methods, Colloids Surf. B Biointerfaces 160 (2017) 117–125.
[22] A. Arslan Yildiz, U.H. Yildiz, B. Liedberg, E.-K. Sinner, Biomimetic membrane platform: fabrication, characterization and applications, Colloids Surf. B Biointerfaces 103 (2013) 510–516.
[23] C. Elie-Caille, O. Fliniaux, J. Pantigny, J.-C. Mazière, C. Bourdillon, Self-assembly of solid-supported membranes using a triggered fusion of phospholipid-enriched proteoliposomes prepared from the inner mitochondrial membrane1, Langmuir 21 (2005) 4661–4668.
[24] S.G. Patching, Surface plasmon resonance spectroscopy for characterisation of membrane protein–ligand interactions and its potential for drug discovery, Biochim. Biophys. Acta 1838 (2014) 43–55.
[25] M. Brändén, S. Dahlin, F. Höök, Label-free measurements of molecular transport across liposome membranes using evanescent-wave sensing, ChemPhysChem 9 (2008) 2480–2485.
[26] I.F. Márquez, M. Vélez, Formation of supported lipid bilayers of charged E. coli lipids on modified gold by vesicle fusion, Domain Decompos. Method. Sci. Eng. XX 2011 (2011) 4 (2017) 461–468.
[27] N.-J. Cho, S.-J. Cho, K.H. Cheong, J.S. Glenn, C.W. Frank, Employing an amphipathic viral peptide to create a lipid bilayer on Au and TiO2, J. Am. Chem. Soc. 129 (2007) 10050–10051.
[28] M.P. Beseničar, A. Bavdek, A. Kladnik, P. Maček, G. Anderluh, Kinetics of cholesterol extraction from lipid membranes by methyl-β-cyclodextrin—a surface plasmon resonance approach, Biochim. Biophys. Acta 1778 (2008) 175–184.
[29] D.G. Villalva, L. Giansanti, A. Mauceri, F. Ceccacci, G. Mancini, Influence of the state of phase of lipid bilayer on the exposure of glucose residues on the surface of liposomes, Colloids Surf. B Biointerfaces 159 (2017) 557–563.
[30] S. Gromelski, A.M. Saraiva, R. Krastev, G. Brezesinski, The formation of lipid bilayers on surfaces, Colloids Surf. B Biointerfaces 74 (2009) 477–483.
[31] E.S. Melby, A.C. Mensch, S.E. Lohse, D. Hu, G. Orr, C.J. Murphy, R.J. Hamers, J.A. Pedersen, Formation of supported lipid bilayers containing phase-segregated domains and their interaction with gold nanoparticles, Environ. Sci. Nano 3 (2016) 45–55.
[32] C. Satriano, G. Lupo, C. Motta, C.D. Anfuso, P. Di Pietro, B. Kasemo, Ferritin-supported lipid bilayers for triggering the endothelial cell response, Colloids Surf. B Biointerfaces 149 (2017) 48–55.
[33] S.M. Maté, R.F. Vázquez, V.S. Herlax, M.A. Daza Millone, M.L. Fanani, B. Maggio, M.E. Vela, L.S. Bakás, Boundary region between coexisting lipid phases as initial binding sites for Escherichia coli alpha-hemolysin: a real-time study, Biochim. Biophys. Acta 1838 (2014) 1832–1841.
[34] R.F.M. de Almeida, A. Fedorov, M. Prieto, Sphingomyelin/phosphatidylcholine/cholesterol phase diagram: boundaries and composition of lipid rafts, Biophys. J. 85 (2003) 2406–2416.
[35] T.B. Creczynski-Pasa, M.A.D. Millone, M.L. Munford, V.R. de Lima, T.O. Vieira, G.A. Benitez, A.A. Pasa, R.C. Salvarezza, M.E. Vela, Self-assembled dithiothreitol on Au surfaces for biological applications: phospholipid bilayer formation, PCCP 11 (2009) 1077–1084.
[36] M.A. Daza Millone, M.E. Vela, R.C. Salvarezza, T.B. Creczynski-Pasa, N.G. Tognalli, A. Fainstein, Phospholipid bilayers supported on thiolate-covered nanostructured gold: in situ raman spectroscopy and electrochemistry of redox species, ChemPhysChem 10 (2009) 1927–1933.
[37] K. El Kirat, S. Morandat, Y.F. Dufrêne, Nanoscale analysis of supported lipid bilayers using atomic force microscopy, Biochim. Biophys. Acta 1798 (2010) 750–765.
[38] S. Garcia-Manyes, G. Oncins, F. Sanz, Effect of ion-binding and chemical phospholipid structure on the nanomechanics of lipid bilayers studied by force spectroscopy, Biophys. J. 89 (2005) 1812–1826.
[39] S. Garcia-Manyes, F. Sanz, Nanomechanics of lipid bilayers by force spectroscopy with AFM: a perspective, Biochim. Biophys. Acta 1798 (2010) 741–749.
[40] S. Garcia-Manyes, L. Redondo-Morata, G. Oncins, F. Sanz, Nanomechanics of lipid bilayers: heads or tails? J. Am. Chem. Soc. 132 (2010) 12874–12886.
[41] R. Leventis, J.R. Silvius, Use of cyclodextrins to monitor transbilayer movement and differential lipid affinities of cholesterol, Biophys. J. 81 (2001) 2257–2267.
[42] E.L. Florin, M. Rief, H. Lehmann, M. Ludwig, C. Dornmair, V.T. Moy, H.E. Gaub, Sensing specific molecular interactions with the atomic force microscope, Biosens. Bioelectron. 10 (1995) 895–901.
[43] D. Nečas, P. Klapetek, Gwyddion: an open-source software for SPM data analysis, Open Phys. (2012) 181.
[44] C.E. Wagner, L.J.A. Macedo, A. Opdahl, Temperature gradient approach for rapidly assessing sensor binding kinetics and thermodynamics, Anal. Chem. 87 (2015) 7825–7832.
[45] D.A. Brown, E. London, Structure and origin of ordered lipid domains in biological membranes, J. Membr. Biol. 164 (1998) 103–114.
[46] A. Melcrová, S. Pokorna, S. Pullanchery, M. Kohagen, P. Jurkiewicz, M. Hof, P. Jungwirth, P.S. Cremer, L. Cwiklik, The complex nature of calcium cation interactions with phospholipid bilayers, Sci. Rep. 6 (2016) 38035.
[47] J.A. De Feijter, J. Benjamins, F.A. Veer, Ellipsometry as a tool to study the adsorption behavior of synthetic and biopolymers at the air–water interface, Biopolymers 17 (1978) 1759–1772.
[48] W.M. Albers, I. Vikholm-Lundin, Nano-bio-sensing, in: Carrara Sandro (Ed.), Surface Plasmon Resonance on Nanoscale Organic Films, Springer, New York, NY, 2011.
[49] E. Stenberg, B. Persson, H. Roos, C. Urbaniczky, Quantitative determination of surface concentration of protein with surface plasmon resonance using radiolabeled proteins, J. Colloid Interface Sci. 143 (1991) 513–526.
[50] M.C. Phillips, D. Chapman, Monolayer characteristics of saturated 1,2-diacyl phosphatidylcholines (lecithins) and phosphatidylethanolamines at the air-water interface, Biochim. Biophys. Acta 163 (1968) 301–313.
[51] H. Xu, J.J. Hill, K. Michelsen, H. Yamane, R.J.M. Kurzeja, T. Tam, R.J. Isaacs, F. Shen, P. Tagari, Characterization of the direct interaction between KcsA-Kv1.3 and its inhibitors, Biochim. Biophys. Acta 1848 (2015) 1974–1980.
[52] A. Erbe, R. Sigel, Tilt angle of lipid acyl chains in unilamellar vesicles determined by ellipsometric light scattering, EPJ E 22 (2007) 303–309.
[53] A. Theisen, C. Johann, M.P. Deacon, S.E. Harding, Refractive Increment Data-book for Polymer and Biomolecular Scientists, Nottingham University Press, Nottingham, 2000.
[54] S. Ip, J.K. Li, G.C. Walker, Phase Segregation of untethered zwitterionic model lipid bilayers observed on mercaptoundecanoic-acid-modified gold by AFM imaging and force mapping, Langmuir 26 (2010) 11060–11070.
[55] C. Montis, S. Busatto, F. Valle, A. Zendrini, A. Salvatore, Y. Gerelli, D. Berti, P. Bergese, Biogenic supported lipid bilayers from nanosized extracellular vesicles, Adv. Biosys. (2018) 1700200.
[56] R. Koynova, M. Caffrey, Phases and phase transitions of the phosphatidylcholines, BBA – Rev. Biomembr. 1376 (1998) 91–145.
[57] J.S. Attwood, Y. Choi, Z. Leonenko, Preparation of DOPC and DPPC supported planar lipid bilayers for atomic force microscopy and atomic force spectroscopy, Int. J. Mol. Sci. (2013) 14.
[58] M.G. Sorci-Thomas, M.J. Thomas, Microdomains, inflammation, and atherosclerosis, Circul. Res. 118 (2016) 679.
[59] Y. Lange, T.L. Steck, Cholesterol homeostasis and the escape tendency (activity) of plasma membrane cholesterol, Prog. Lipid Res. 47 (2008) 319–332.
[60] T. Irie, M. Otagiri, M. Sunada, K. Uekama, Y. Ohtani, Y. Yamada, Y. Sugiyama, Cyclodextrin-induced hemolysis and shape changes of human erythrocytes in vitro, J. Pharm. Dyn. 5 (1982) 741–744.
[61] C.A. López, A.H. de Vries, S.J. Marrink, Computational microscopy of cyclodextrin mediated cholesterol extraction from lipid model membranes, Sci. Rep. 3 (2013) 2071.
[62] Y. Lange, T.L. Steck, Active membrane cholesterol as a physiological effector, Chem. Phys. Lipids 199 (2016) 74–93.